Growth of InP Nanostructures via Reaction of Indium Droplets with Phosphide Ions: Synthesis of InP Quantum Rods and InP−TiO 2 Composites

ARTICLE *in* JOURNAL OF THE AMERICAN CHEMICAL SOCIETY · APRIL 2004

Impact Factor: 12.11 · DOI: 10.1021/ja039311a · Source: PubMed

J|A|C|S
ARTICLES
Published on Web 02/04/2004

Growth of InP Nanostructures via Reaction of Indium Droplets with Phosphide Ions: Synthesis of InP Quantum Rods and InP−TiO_2 Composites

Jovan M. Nedeljković, Olga I. Mićić,* S. Phillip Ahrenkiel, Alex Miedaner, and Arthur J. Nozik

Contribution from the National Renewable Energy Laboratory, 1617 Cole Boulevard, Golden, Colorado 80401

Received October 29, 2003; E-mail: olga_micic@nrel.gov

Abstract: InP quantum rods were synthesized via the reaction of monodispersed colloidal indium droplets with phosphide ions. In^0 droplets, which do not act as a catalyst but rather a reactant, are completely consumed. The excess electrons that are produced in this reaction are most likely transferred to an oxide layer at the indium surface. For the synthesis of InP quantum rods with a narrow size distribution, a narrow size distribution of In^0 particles is also required because each indium droplet serves as a template to strictly limit the lateral growth of individual InP nanocrystals. Free-standing quantum rods, 60, 120, or 150 Å in diameter, with aspect ratios of 1.6−3.5, and without the residual metallic catalyst at the rod tip, were synthesized from the diluted transparent solution of metallic indium particles. The same approach was used to synthesize InAs quantum rods. A photoactive InP−TiO_2 composite was also prepared by the same chemical procedure; InP nanocrystals grow as well-defined spherical or slightly elongated shapes on the TiO_2 surface.

Introduction

Colloidal III−V semiconductor nanocrystals (quantum dots, QDs) have been the subject of intensive experimental and theoretical study because of the rich phenomena associated with quantum confinement. Most studies have involved spherical-like nanocrystals, but both shape and size control the electrical and optical properties of nanocrystals. The effects of the nanocrystal shape have not received much attention until recently, because colloidal synthetic methods for their preparation have not been available. Cylindrical or one-dimensional structures of nanocrystals, namely, quantum rods (QRs) and quantum wires (QWs), have potential technological advantages over QD spheres in such applications as photovoltaic cells, lasers, and linearly polarized emission. Studies of QRs and QWs have recently been reported.[1−7] It has been shown,[8] for example, that CdSe QRs, when organized into ordered arrays, exhibit improved electronic transport compared to self-assembled QDs; this is attributed to preferred charge transport along the long axis of the QR.

Quantum rods synthesized by colloidal methods with a surfactant stabilizer are usually soluble in organic solvents if they have short lengths; quantum wires with a very large aspect ratio are generally insoluble. So far, the growth of soluble quantum rods using surfactants has been limited primarily to the wurtzite II−VI semiconductors. These QRs have been synthesized by controlling the difference in growth rate among various crystallographic faces[2] or by rod growth from oriented and aligned individual quantum dots.[9] Cheon et al.[10] recently synthesized the wurtzite structure of GaP nanorods, although GaP has a large difference in total energy between the wurtzite and zinc blende phases. They used different stabilizers to affect a crystallographic phase transformation from the zinc blende to the wurtzite structure. However, we found that their approach cannot be applied to the growth of InP nanocrystals[11] because the indium metal that is formed by thermal decomposition of the analogous precursor used for GaP is a better catalyst for anisotropic growth of zinc blende InP crystallites than is gallium metal.

For materials with a zinc blende cubic lattice, the solution−liquid−solid (SLS) mechanism[12] with liquid metallic droplets as the catalyst has been widely used to synthesize wirelike crystallites. The SLS method is analogous to the vapor−liquid−

(1) Lieber, C. M. *Solid State Commun.* **1998**, *107*, 607.
(2) Peng, X.; Manna, L.; Yang, W.; Wickham, J.; Scher, E.; Kadavanich, A.; Alivisatos, A. P. *Nature* **2000**, *404*, 59.
(3) Hu, J.; Li, L.; Yang, W.; Manna, L.; Wang, L.; Alivisatos, A. P. *Science* **2001**, *292*, 2063.
(4) Htoon, H.; Hollingsworth, J. A.; Malko, A. V.; Dickerson, R.; Klimov, V. I. *Appl. Phys. Lett.* **2003**, *82*, 4776.
(5) Kazes, M.; Lewis, D. Y.; Ebenstein, Y.; Mokari, T.; Banin, U. *Adv. Mater.* **2002**, *14*, 317.
(6) Wu, Y.; Yang, P. *J. Am. Chem. Soc.* **2001**, *123*, 3165.
(7) Murray, C. B.; Sun, S.; Gaschler, W.; Doyle, H.; Betley, T. A.; Kagan, C. R. *IMB J. Res. Dev.* **2001**, *45*, 47.
(8) Huynh, W. U.; Dittmer, J. J.; Alivisatos, A. P. *Science* **2002**, *295*, 2425.
(9) Tang, Z.; Kotov, N. A.; Giersig, M. *Science* **2002**, *297*, 237.
(10) Kim, Y.-H.; Jun, Y.-w.; Jun, B.-H.; Lee, S.-M.; Cheon, J. *J. Am. Chem. Soc.* **2002**, *124*, 13656.
(11) Ahrenkiel, S. P.; Micic, O. I.; Miedaner, A.; Curtis, C. J.; Nedeljkovic, J. M.; Nozik, A. J. *Nano Lett.* **2003**, *3*, 833.
(12) Trentler, T. J.; Goel, S. C.; Hickman, K. M.; Viano, A. M.; Chiang, M. Y.; Beatty, A. M.; Gibbons, P. C.; Buhro, W. E. *J. Am. Chem. Soc.* **1997**, *119*, 2172.

10.1021/ja039311a CCC: $27.50

solid (VLS) method,[1] which generates single-crystal wires in relatively large quantities. Very recently, quantum rods and wires of InAs[13] and InP[11,13,14] with controllable diameters and excellent crystallinity were synthesized by the SLS method. However, the fabrication of III−V semiconductor QRs remains difficult regarding the control of size, length, and size uniformity. Another difficulty with QRs synthesized by the SLS method is residual metallic catalyst spherules (Au, In) present at the rod tip. The presence of these metal catalyst particles interferes with measurements of the optical and electronic properties of the QRs.

Here, we report a novel chemical route to the growth of pure InP QRs without any residual metallic catalyst. We use colloidal monodispersed metallic indium droplets as a reactant, in which phosphine molecules are subsequently adsorbed and then bonded to In atoms to yield InP QRs at low temperatures (110−220 °C). The synthesis is analogous to the aerosol synthesis of III−V nanocrystals at high temperature, termed aerotaxy, which was developed by Samuelson et al.,[15,16] and in which evaporated metal at about 1000 °C reacts with group-V hydrides to yield corresponding binary III−V nanocrystals. The first step in our procedure is the synthesis of colloidal monodispersed zerovalent indium particles that we prepared by thermal decomposition of organoindium compounds in organic solvent in the presence of a colloidal stabilizer. As a source of phosphine molecules, we used tris(trimethylsilyl)phosphine ($P(SiMe_3)_3$) that, in the presence of protonic agents, hydrolyzes into PH_3. The novelty of this procedure is that the diameter and length of the final InP QRs is self-limited by the size of the introduced monodispersed In^0 droplets at low temperature. As expected, the absorption and photoluminescence spectra of the InP nanorods exhibit a blue shift with respect to the bulk band gap (1.35 eV) that is due to quantum confinement.

Experiment

Synthesis of Colloidal Indium Nanoparticles. All compounds used in this work are extremely sensitive to oxygen and moisture, and they were manipulated in a Schlenk line or glovebox under rigorously air- and water-free conditions. Tri-*tert*-butylindium ($In(t\text{-But})_3$) was synthesized by an established literature method.[17] Monodisperse indium nanoparticles were synthesized by an organometallic route using $In(t\text{-But})_3$, cyclopentadienylindium(I) (C_5H_5In, Strem), or pentamethylcyclopentadienylindium(I) ($(CH_3)_5C_5In$, Strem) as precursors. Synthesis of indium nanoparticles of 190-Å diameter is based on thermal decomposition of 30 mg of $In(t\text{-But})_3$ in 4 mL of trioctylphosphine (TOP, Aldrich) containing 30 mg of hexadecylamine (HDA, Aldrich) at 140 °C for 45 min. The solution turns brown when indium nanoparticles are formed. For smaller nanoparticles, C_5H_5In or $(CH_3)_5C_5In$ is used; it spontaneously decomposes and yields indium particles. C_5H_5In has been used previously to synthesize In^0 nanoparticles with a narrow size distribution.[18] Indium particles 65 Å in diameter were synthesized by decomposition of 5−10 mg of C_5H_5In in 10 mL of toluene containing 0.1 mL of trioctylamine (TOA) in the absence of light at room temperature. Heating the same solution at 50 °C produces monodispersed indium particles that are about 80 Å in diameter. Similarly, indium nanoparticles of 150 Å were prepared by thermal decomposition of 26 mg of $(CH_3)_5C_5In$ in 4 mL of TOP containing 30 mg of HDA at 80 °C. An increase in temperature under the same condition yields monodispersed indium particles with larger diameters. An as-synthesized In^0 solution was used for the synthesis of QRs. For TEM measurements, In^0 particles are precipitated from the solution with acetone and redissolved in toluene and loaded on TEM grids.

Synthesis of InP Nanorods Using Metallic Indium Nanoparticles as Starting Material. InP nanorods were synthesized by reacting $P(SiMe_3)_3$ with In^0 nanoparticles dispersed in organic solvents. An as-prepared solution that contained In^0 nanoparticles (1−3 mg) was diluted with TOP for high-temperature treatment or with 10 mL of toluene for low-temperature treatment in the presence of 30 mg of HDA and then mixed with 20−65 mg of $P(SiMe_3)_3$ in a drybox. For preparation of InP nanorods at room temperature, a solution containing 1 mg of In^0 in 10 mL of toluene was used and protonic agents (0.2 mL), methanol or thiophenol (PhSH), were added to hydrolyze the $P-SiMe_3$ bond and to form PH_3. Nanowires are formed when the solution is mixed and immediately heated at 220 °C for 2 min. Short nanorods were prepared when a solution of 80-Å indium particles that contained 1 mg of In^0 were mixed with 30 mg of $P(SiMe_3)_3$ in 2.5 mL of TOP, 2.5 mL of toluene, and 30 mg of HDA and heated for 2 h at 110 °C in a closed system saturated with nitrogen. The reaction cell was open to nitrogen atmosphere, and 4 mg of $InCl_3$ dissolved in 1 mL of TOP was slowly added. QRs that are synthesized in a large excess of $P(SiMe_3)_3$ exhibit slightly increased emission after addition of $InCl_3$. The shape of a small portion of the particles is round. They can be removed from the system by size-selective precipitation. InP nanorods of 120 Å in diameter were prepared by mixing 1 mg of 150-Å indium particles dispersed in 1 mL of TOP containing 30 mg of HDA with 50 mg of $P(SiMe_3)_3$ in a closed system within a glovebox; after 2 days, 0.1 mL of PhSH was added and the mixture was left at room temperature for an additional 3 days. This solution was then heated at 220 °C for 1 day.

Formation of the InP nanorods is accompanied by the appearance of an intense brown color because InP nanorods have a larger extinction coefficient compared to In QDs. During the synthesis, all the excess volatile phosphorus compounds were collected with a trap of aqueous sodium hydroxide solution that was placed at the end of the nitrogen line. When the synthesis was finished, the trap solution was oxidized with commercial bleach.

After heating, the raw colloid consisting of InP nanorods was diluted with toluene and precipitated with methanol. The precipitate was dissolved in pyridine and reprecipitated in excess methanol. The resulting precipitate was dissolved in 1 wt % HDA in chloroform to obtain clean samples.

InP−TiO_2 Composites. TiO_2 nanorods were synthesized in a two-step process. First, trititanate nanotubes of $Na_2Ti_3O_7$ were prepared via a hydrothermal chemical processes described in the literature.[19] We synthesized trititinate nanotubes of about 90 Å in diameter and one thousand to several thousand angstroms in length. The nanotubes have open-end and multiwall morphology. We converted these materials into the H-form of trititanate, $H_2Ti_3O_7$, by substituting Na^+ with H_3O^+ in HCl solution. These $H_2Ti_3O_7$ nanotubes were used for the preparation of anatase TiO_2 nanorods. Anatase TiO_2 nanorods were synthesized by heat treatment of the $H_2Ti_3O_7$ nanotubes at 250 °C for 1 h in supercritical water. To the best of our knowledge, there is no prior literature describing the formation of anatase TiO_2 nanorods using this approach. The solid product was washed with hot water several times and vacuum-dried at 60 °C overnight. For preparation of the InP−TiO_2 composite, TiO_2 powder (20 mg) was dispersed in 3 mL of 9-octadecene and 0.5 mL of toluene by sonication. The In^0 particles (1−5 mg) were added to TiO_2 and stirred for 3 days at room temperature

(13) Kan, S.; Mokari, T.; Rothenberg, E.; Banin, U. *Nat. Mater.* **2003**, *2*, 155.
(14) Yu, H.; Li, J.; Loomis, R. A.; Wang, L.-W.; Buhro, W. E. *Nat. Mater.* **2003**, *2*, 517.
(15) Deppert, K.; Magnusson, M. H.; Samuelson, L.; Malm, J.-O.; Svensson, C.; Bovin, J.-O. *J. Aerosol Sci.* **1998**, *29*, 737.
(16) Deppert, K.; Bovin, J.-O.; Magnusson, M. H.; Malm, J.-O.; Svensson, C.; Samuelson, L. *Jpn. J. Appl. Phys.* **1999**, *38*, 1056.
(17) Bradley, D. C.; Frigo, D. M.; Hursthouse, M. B.; Hussain, B. *Organometallics* **1988**, *7*, 1112.
(18) Soulantica, K.; Maisonnat, A.; Fromen, M.-C.; Casanove, M.-J.; Lecante, P.; Chaudret, B. *Angew. Chem., Int. Ed.* **2001**, *40*, 448.
(19) Chen, Q.; Zhou, W.; Du, G.; Peng, L.-M. *Adv. Mater.* **2002**, *14*, 1208.

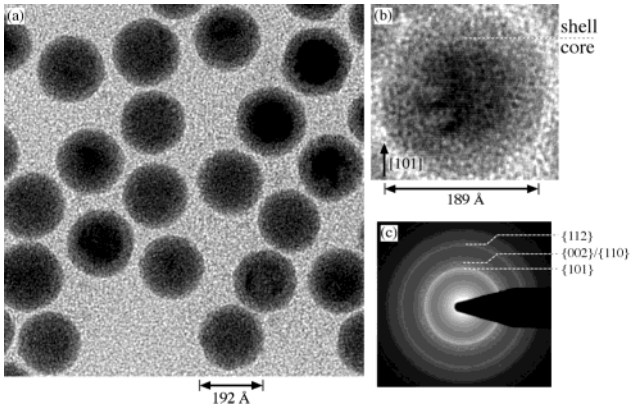

Figure 1. TEM images of 190-Å In^0 nanoparticles prepared by thermal decomposition of In(*t*-But)$_3$ in TOP/HDA at 140 °C showing (a) an ensemble, (b) a high-resolution TEM image of an In^0 nanoparticle with a tetragonal core and an amorphous/polycrystalline shell, and (c) electron diffraction pattern.

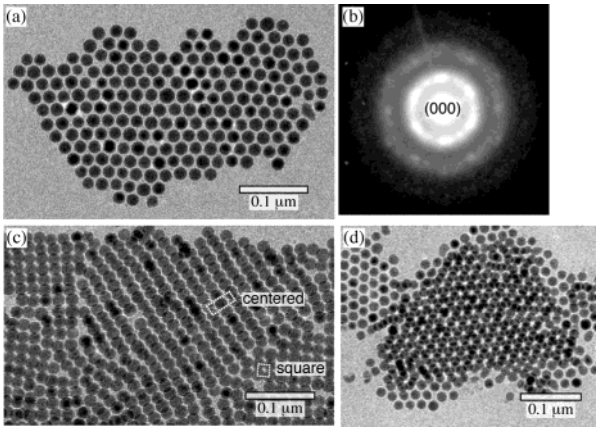

Figure 2. TEM images of 190-Å In^0 nanoparticles showing (a) formation of a 2-D hexagonal superstructure, (b) the electron diffraction pattern of the 2-D hexagonal superstructure, (c) formation of a 2-D square superstructure, and (d) formation of a 3-D hexagonal superstructure.

to adsorb In^0 particles on the TiO_2 surface. After that, 45 mg of $P(SiMe_3)_3$ was added and then heated 1 day at 220 °C. The solid product was washed with chloroform, methanol, and acetone several times.

Characterization. Optical absorption spectra were collected at room temperature using a Cary 5E UV−vis−near-IR spectrophotometer. Photoluminescence spectra were obtained at room temperature using an SPEX Fluorolog-2 spectrometer.

Colloidal samples were deposited on C-coated Cu grids for microstructural analysis. Characterization was carried out on a Philips CM30 TEM operated at 200 kV. Bright-field and lattice images were acquired with an objective aperture that admitted contributions from low-index reflections. Selected-area patterns were acquired with an aperture having a projected diameter of approximately 7 μm in the image plane. EDX spectra were acquired with a Kevex Li-drifted Si detector using the Emispec ES Vision software.

X-ray diffraction (XRD) patterns were acquired on a Scintag $\times 1$ diffractometer using Cu Kα radiation.

Discussion and Results

Synthesis of Metallic Indium Particles. We have developed a method for the synthesis of monodispersed In^0 particles. A narrow size distribution of In^0 particles is required for the synthesis of InP QRs with a narrow distribution of diameters because each indium droplet serves as a template to strictly limit the lateral growth of individual InP QRs.[15] Nanocrystals of noble and magnetic metals have been studied intensively, and they are usually synthesized by thermal decomposition of organometallic precursors. However, there are only a few reports on the synthesis of metallic indium particles. They have been prepared previously by the reduction of $InCl_3$ with alkalides[20] and recently by decomposition of C_5H_5In in the presence of stabilizers at room temperature.[18] We synthesized indium particles with diameters of 190, 65, and 150 Å by thermal decomposition of three different organometallic precursors, In(*t*-But)$_3$, C_5H_5In, and $(CH_3)_5C_5In$, respectively. Figure 1 shows spherical 190-Å metal indium particles that were obtained by the thermal decomposition of In(*t*-But)$_3$ in TOP/HDA solution.

The nanoparticles have a tetragonal crystal core and an amorphous polycrystalline shell (Figure 1b). Although it is well-documented that the melting point of solid materials will be greatly reduced below that of the bulk when its dimensions approach a few nanometers, and indium is a low-melting-point

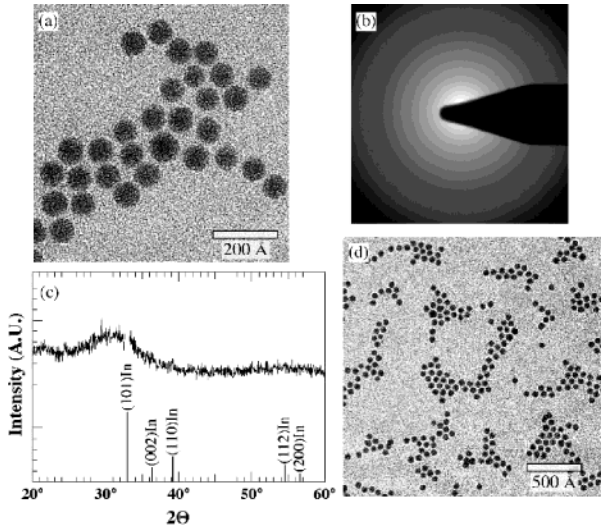

Figure 3. TEM images showing (a) an ensemble of 65-Å In^0 nanoparticles prepared by decomposition of C_5H_5In in TOA/toluene at room temperature, (b) electron diffraction, (c) an X-ray diffraction pattern, and (d) a low-resolution image.

metal (mp 157 °C), we found that the 190-Å In^0 particles do not melt at room temperature. Electron diffraction data (Figure 1c) show that the core of the 190-Å indium particles consists of the tetragonal phase of solid metal indium. This result is in agreement with previously published results for the size-dependent melting point of indium metal particles with diameters of 67, 50, and 40 Å and with melting points of +70, +35, and −4 °C, respectively.[21]

The 190-Å indium nanoparticles have an extremely narrow size distribution (<5%) and are capable of forming 2-D and 3-D ordered superstructures, as can be seen in Figure 2. The superstructure diffraction rings were also detected (Figure 2b); the hexagonal superstructure is dominant, although a cubic superstructure can also be noticed.

A TEM image of metallic indium nanoparticles prepared with C_5H_5In as a precursor is shown in Figure 3. The spontaneous decomposition of C_5H_5In at room temperature yields well-separated monodispersed indium particles with an average diameter of 65 Å and a size distribution of about 5−6%.

(20) Tsai, K.-L.; Dye, J. L. *J. Am. Chem. Soc.* **1991**, *113*, 1650.

(21) Coombes, J. *J. Phys. F: Metal Phys.* **1972**, *2*, 441.

This is in agreement with a previous synthesis of narrow-size-distributed In^0 nanoparticles using a C_5H_5In precursor.[18] Figure 3c shows the presence of the broad low-index diffraction ring, indicating that the 65-Å particles still have a solid phase. We found that indium nanoparticles oxidize extremely easily in air. EDX analysis shows that oxygen is also present in the In^0 particles. The presence of oxide can be detected in our samples by observing a shoulder at 470 nm in the absorption spectrum and an emission peak at about 500 nm (the band gap of In_2O_3 is 2.6 eV). The absorbance of indium particles monotonically increases with decreasing wavelength. A surface oxide can be formed because of the presence of trace water in the organic solvent, as well as exposure of the sample to air prior to introduction into the microscope. We also found that In^0 easily converts to In_2O_3 when In^0 particles are exposed to oxygen at 220 °C for several hours in TOA/HDA solution. The dark brown solution turned yellow. An XRD pattern of the powder sample shows cubic In_2O_3 without any trace of metallic indium; the yellow precipitate can be partially dissolved in chloroform.

InP Nanorods Formed by Reaction of Metallic Indium with Phosphine. We developed a new approach to the synthesis of colloidal InP QRs. All QRs synthesized in this work are in the strong confinement regime because the Bohr diameter of InP bulk excitons is about 200 Å. Metallic indium particles were used as the starting material, which subsequently reacted with P^{3-} or H_3P to form InP QRs. This method can also be used for the preparation of other indium-V semiconductor quantum rods when group-V hydrides are used instead of H_3P. For the preparation of InP rods, we used $P(SiMe_3)_3$ as a source of phosphide ions, which, in the presence of protonic agents (methanol, PhSH, or RNH_2), hydrolyzes into PH_3 and then is neutralized with HDA (RNH_2) to form $(RNH_3^+)_3P$ salt. We found that, even at room temperature, metallic indium reacts with P^{3-} or H_3P to produce one-dimensional growth of InP QRs:

$$In^0 + P^{3-} = InP_{rod} + 3e^- \quad (1)$$

Three electrons are produced in this reaction; they are most likely consumed in the reduction of the oxide layer at the indium surface and also by solvent impurities. This reducing environment also protects against further oxidation during the InP QR growth process.

When the temperature is higher than the melting point of In^0 nanoparticles, the first step is the dissolution of phosphide into In^0 droplets; this is most likely followed by transfer of electrons to an oxide layer at the melted indium/indium oxide interface. Atomic phosphorus reacts with indium to form InP molecules. The nucleation occurs in supersaturated droplets, and the metallic indium surface is the location where axial InP growth originates. The growth process still undergoes a solution−liquid−solid mechanism which is widely used for the growth of III−V nanowires. In the growth process by the SLS mechanism three well-defined stages have been clearly identified: dissolution, nucleation, and axial growth. Nanowires preferentially elongate perpendicular to crystallographic {111} planes since the growth rate decrease in the order (111)A > (001) > (110) > (111)B for zinc blende cubic III−V semiconductors.[16,22] In our experiments In^0 droplets are not a catalyst but a reacting material that is completely consumed during reaction with the phosphide ions. Preferential 1-D growth occurs as long as liquid indium is present. The simple reaction 1 yields pure InP as the final products. To the best of our knowledge, there is no prior literature describing the formation of free-standing zinc blende III−V semiconductor nanorods or nanowires with no residual metallic catalyst remaining in the final product.

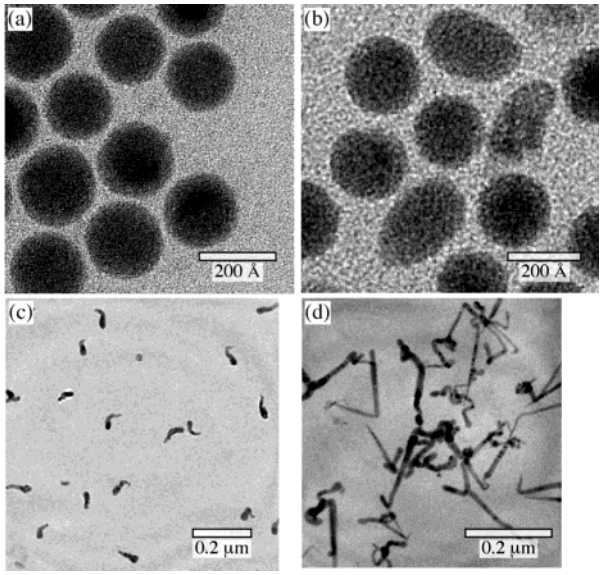

Figure 4. TEM images showing the growth of InP nanorods at room temperature from (a) 190-Å In^0 nanoparticles immediately after being dispersed in a toluene solution of $P(SiMe_3)_3$, PhSH, and HDA and after (b) 1 and (c) 3 days. (d) TEM image of InP nanorods obtained by mixing 190-Å In^0 nanoparticles and $P(SiMe_3)_3$ at room temperature and immediately heating at 220 °C.

Reaction is most likely one of the sequence of complex growth steps in the solvothermal synthesis of InP nanowires from $InCl_3$ and P_n in the presence of a strong reducing agent.[23] Under these conditions, $InCl_3$ and P_n reduce to In^0 and P^{3-}, respectively, producing the same starting materials indicated in reaction 1. Solvothermal synthesis utilizes a solvent under pressure and temperature above the critical point in order to increase the solubility of the solid reactants and to speed up reaction between solids. However, in our case, reaction 1 occurs even at room temperature because colloidal In^0 particles and $P(SiMe_3)_3$ are soluble in organic solvents and the whole growth process of InP QRs can be controlled by the concentration of In^0 particles and the temperature in the reaction cell. We found that reaction 1 takes place even at room temperature as a very slow process and is completely finished only after several days.

Parts a−c of Figure 4 show the development of the changes in shape with time of 190-Å indium particles that are exposed to $P(SiMe_3)_3$ at room temperature as InP QRs grow from the In^0 surface. The growth of InP rods was observed from indium particles immersed in a toluene solution of $P(SiMe_3)_3$, methanol (or PhSH), and HDA. After 1 day (Figure 4b), most of particles are spherical, but some of them show shape changes and start to exhibit a rodlike shape. After 3 days in excess $P(SiMe_3)_3$, metallic indium is completely converted into InP QRs at room temperature; lower resolution TEM images (Figure 4c) dem-

(22) Seidel-Salinas, L. K.; Jones, S. H.; Duva, J. M. *J. Cryst. Growth* **1992**, *123*, 575.
(23) Yan, P.; Xie, Y.; Wang, W.; Liu, F.; Qian, Y. *J. Mater. Chem.* **1999**, *9*, 1833.

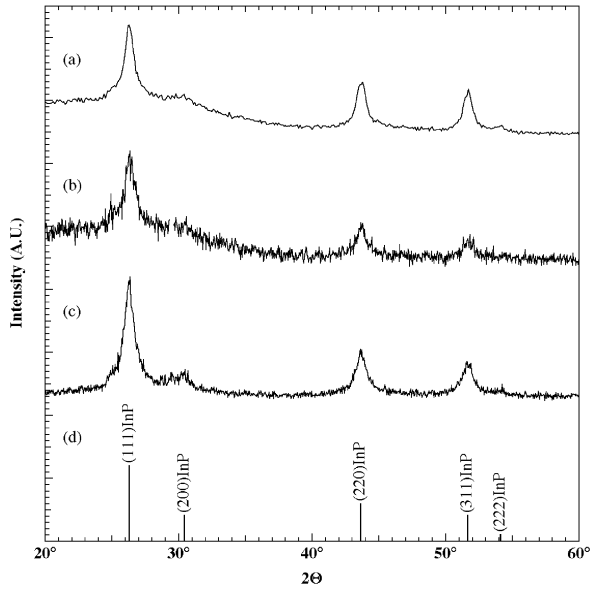

Figure 5. X-ray diffraction pattern for as-prepared InP samples after heating 190-Å In^0 nanoparticles and $P(SiMe_3)_3$ in HDA/TOP at (a) 320 °C for 10 s, (b) 220 °C for 2 min, and (c) 140 °C for 90 min. (d) Powder diffraction lines for zinc blende InP.

onstrate the formation of well-separated free-standing rods with a tadpole-like shape. Each indium droplet strictly limits the lateral growth of individual InP rods. Soluble free-standing QRs can be prepared only from a diluted solution of In^0 droplets (0.1−0.2 mg of In^0/(1 mL of solvent)). Concentrated solution favors formation of nanorods with many arms (2 mg of In^0/(1 mL of solvent)). The presence of In^0 could not be detected by XRD or in electron diffraction measurements after 3 days of contact. EDAX analysis of such particles reveals their composition to be close to 50% In and 50% P.

The 190-Å In^0 particles that do not melt at room temperature can also yield InP QRs. This is because before bulk melting occurs, local surface melting at the amorphous polycrystalline shell (Figure 1b) and atomic diffusion at the surface can take place at lower temperatures, and this is sufficient to form the reaction center and to start the reaction with phosphine. Now a question arises: how can reaction 1 proceed in growing InP in one direction until there is complete consummation of the well-crystallized solid In^0 core? One possible explanation is that P^{3-} slowly corrodes In^0 particles with time, forming InP monomer and small clusters, and at the same time small fragments of indium reach its melting point at room temperature. Molten indium penetrates to the surface and increases the In^0 reaction center and slowly increases the diameter of InP rod. The final process is the complete conversion of In^0 into InP forming a large spherical tip. The final product, indium-free QRs in Figure 4c, have the diameter that increases from tail to tip forming a tadpole-like shape. It is characteristic that only one nucleation event per In^0 particle occurs and yields QRs. Formation of a secondary nucleation center at the same time probably requires more energy[6] and does not occur in dilute solutions at room temperature.

Higher temperature is required for the synthesis of QRs with a well-developed crystal structure. When In^0 and $P(SiMe_3)_3$ are mixed at room temperature and then immediately heated to 220 °C, QRs form immediately (Figure 4d); QRs of various shapes are evident.

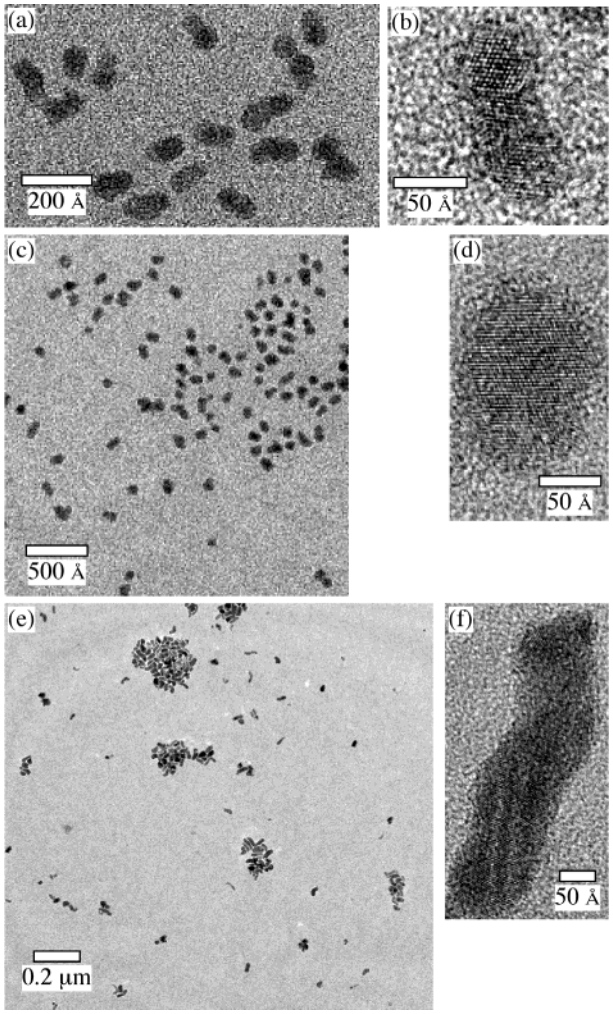

Figure 6. TEM images showing InP QRs: (a−c) 60-Å diameter QRs with aspect ratios of 1.4−2.5 prepared from a solution of 80-Å In^0 particles 110 °C; (d−f) 120-Å diameter QRs with aspect ratios of 1.6−3.3 prepared from a solution of 150-Å In^0 particles that are mixed with $P(SiMe_3)_3$ at room temperature and then heated 220 °C. (b, d, f) High-resolution images of the individual QRs.

For the samples formed at 140, 220, and 320 °C but with different annealing times, the well-resolved X-ray diffraction pattern (Figure 5) with peaks corresponding to (110), (200), (220), and (311) planes precisely matches the zinc blende crystal structure of bulk InP. Crystalline domain sizes determined from the line widths of the diffraction peaks are somewhat smaller than those obtained by TEM measurements. The particle size was calculated from the (111) X-ray diffraction line width $B = \Delta(2\theta)$, taken as the full width at half-maximum (fwhm), and using the Scherrer formula with $K = 0.9$. Strain contributions to the peak broadening and corrections due to particle shape were not considered and may account for some of the discrepancy between the particle size determined by XRD as compared to TEM. For a sample formed at 90 °C for 5 h, the diffraction peaks are extremely weak (they are not present in Figure 5).

Figure 6 shows TEM images of 60- and 120-Å InP quantum rods. The free-standing short QRs, with 60-Å diameter and aspect ratios of 1.4−2.5, were prepared from a solution of 80-Å In^0 particles at 110 °C (Figure 6a−c). Protonic reagents, MeOH or PhSH, were not added to this solution. Under this condition, elimination of the -$SiMe_3$ group from $P(SiMe_3)_3$ is too slow; this reduces the InP growth rate, producing a more uniform

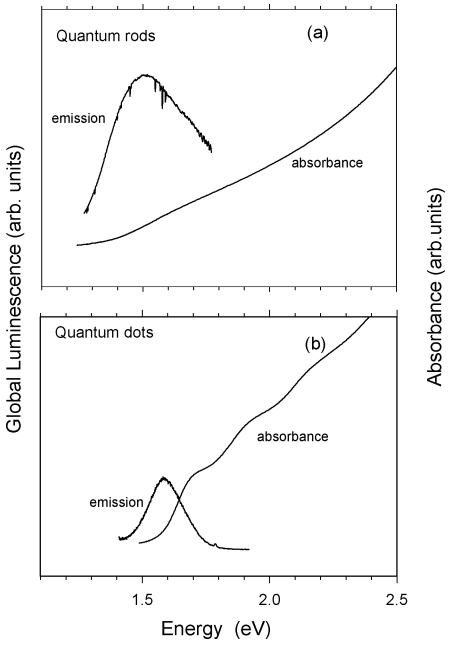

Figure 7. Room-temperature absorption and photoluminescence spectra of (a) InP quantum rods with diameter ~ 60 Å and length ~ 120 Å. (b) InP QDs with a diameter of 60 Å.

diameter along the same quantum rod. Quantum rods in Figure 6 exhibit a characteristic shape with a spherical tip and a short tail. These rods probably show how the growth process occurs: nucleation of InP in a short tail, short axial grow, and complete solidification of melted indium droplets into InP with a nearly spherical shape. A similar shape was observed in situ during the early-stage growth of Ge nanorods on melted Au particles.[6] QRs with diameters of 120 Å and aspect ratios of 1.6−3.5 were prepared using 150-Å In^0 particles. They have diameters about 20% smaller than the In^0 particles. Standard deviations of 10−15% for the diameter and 30% for the length were found for QRs with 60-Å diameters (Figure 6a,c); a slightly broader distribution (Figure 6e) was found for QRs with a diameter of 120 Å.

Analysis by TEM revealed that the diameter and length of the nanorods are self-limited by the size of introduced In^0 particles. The difference in density between InP (4.81 g cm^{-3}) and indium (7.3 g cm^{-3}) translates to a 1.92 volume ratio of InP rods to In^0 spheres. Then, taking into account that the QR diameter is 20% smaller than the In^0 spheres, rods that grow in one dimension will have an aspect ratio of 2.5. This is in relatively good agreement with values estimated from TEM measurements. InP is a polycrystalline material with many stacking faults, as can be seen in Figure 6b,d,f. The crystallization can be improved when nanorods are allowed to age at higher temperatures.

Quantum rods with diameters of 30−80 Å are soluble as colloids and form a transparent colloidal solution. Absorption and emission spectra have a broad band because of a wide distribution in diameter and length, as can be seen in Figure 7a. For the sample of QRs with 60-Å diameters and 120-Å lengths, the photoluminescence peak is at about 1.5 eV. As expected, it is red-shifted when compared to 60-Å diameter InP quantum dots (Figure 7b). In the InP QRs, the length is still in a strong quantum confinement regime (Bohr diameter is 200 Å), and both diameter and length modify the optical properties.

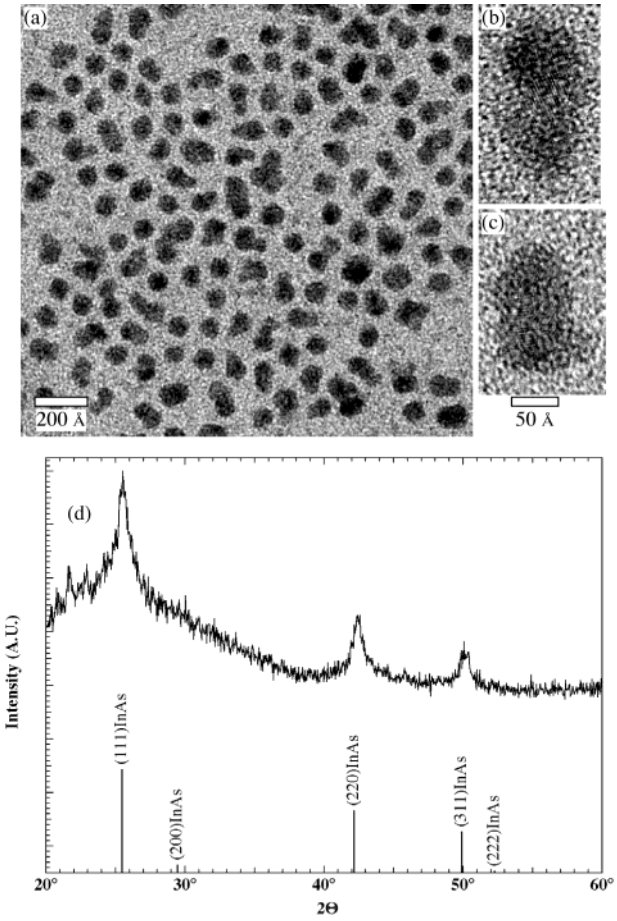

Figure 8. TEM images showing the InAs QRs of about 70 Å in diameter and about 150 Å in length: (a) an ensemble, (b, c) high-resolution images of individual QRs, and (d) an X-ray diffraction pattern for as-prepared InAs sample.

The photoluminescence spectrum is weak and slowly loses intensity after several days and shifts to the UV region, indicating that a surface oxidation process (anodic dissolution) has taken place. InP QRs are not well-passivated since they are synthesized in excess of $P(SiMe_3)_3$ and stabilizers HDA, TOA, and TOP do not coordinate the phosphide ions but rather the indium ions on the QR surface. Better passivation of the nanorod surface and a narrower distribution of length are needed for more precise studies of the optical properties of InP QRs.

The same approach to synthesis can also be used to grow InAs QRs. Figure 8 shows TEM images of InAs QRs synthesized by the same procedure when $As(SiMe_3)_3$ is used instead of $P(SiMe_3)_3$ and the condition for synthesis is the same as those for InP rods present in Figure 6a−c. Colloidal zinc blende InAs QRs were prepared with diameters of about 70 Å and lengths of 100−200 Å. These InAs QRs are in the strong confinement regime because the Bohr diameter is about 700 Å. We estimated the band gap for these QRs to be about 0.8 eV from the optical spectra.

Growth of InP Nanocrystals on TiO_2 Rods. The same chemical procedure can be used to deposit InP on different supporting materials. We synthesized in situ InP nanocrystals on TiO_2 nanorod surfaces by reacting In^0 with H_3P. In these experiments, we wanted to develop the synthesis of the InP−TiO_2 composite that could be used as photoactive electrodes in photoelectrochemical solar cells. Photosensitization of nano-

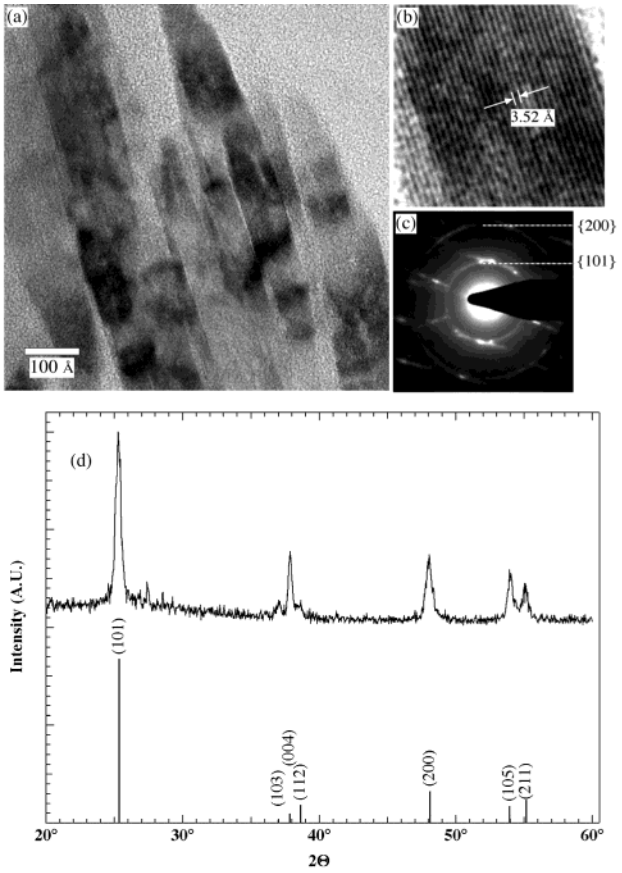

Figure 9. TEM images of anatase TiO_2 nanorods that were synthesized by heat treatment of $H_2Ti_3O_7$ nanotubes at 250 °C for 1 h in supercritical water: (a) an ensemble, (b) a single TiO_2 nanorod, and (c) electron diffraction. (d) X-ray diffraction pattern of TiO_2 nanorods.

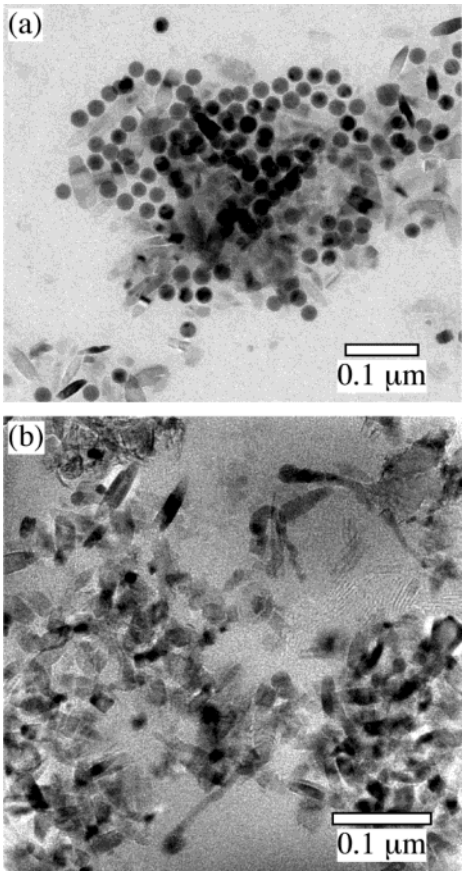

Figure 10. TEM images of InP nanocrystals synthesized on the TiO_2 nanorod surface by reaction of In^0 with H_3P at (a) room temperature and (b) 220 °C.

crystalline TiO_2 semiconductor electrodes by adsorbed semiconductor nanocrystals has been studied previously.[24−27] The bulk InP (band gap is 1.35 eV) absorbs light from the near-IR, through the visible, and to the UV region, and the conduction band has a favorable position for injection of photogenerated electrons into TiO_2.

Anatase TiO_2 nanorods were synthesized by heat treatment of $H_2Ti_3O_7$ nanotubes in supercritical water. Figure 9 shows TEM images of the as-prepared TiO_2 nanorods. A large quantity of pure TiO_2 nanorods with nearly uniform diameters around 10 and 90 nm in length can be clearly seen. In Figure 9b, the X-ray diffraction pattern shows the anatase phase of TiO_2 crystal. The next synthetic step involved depositing InP quantum rods on the TiO_2 nanorod surface by reaction of In^0 with H_3P. Figure 10 shows InP nanocrystals at TiO_2 nanorods. Round InP particles are formed at room temperature after several days (Figure 10a), and InP with a slightly elongated shape (Figure 10b) is formed when In^0-TiO_2 and $P(SiMe_3)_3$ solutions are heated at higher temperature (220 °C). It seems that when In^0 droplets are fixed on the substrate, growth of InP in only one direction is limited and InP nanocrystals of round or slightly elongated shapes are formed. Synthesis of an $InP-TiO_2$ composite illustrates that a simple reaction between In^0 droplets and H_3P can also be used to grow in-situ InP on different supporting materials. Synthesis of $InP-TiO_2$ composite seems to work although the synthesis material is far from being homogeneous in morphology and size, and free InP nanocrystals are also present in the sample (Figure 10b). With the synthesis of $InP-TiO_2$ composites, we hope to obtain better electric contact between InP and TiO_2 and better electron−hole separation inside the $InP-TiO_2$ nanorods. Future work will be directed toward the study of charge relaxation and separation in $InP-TiO_2$ nanorods.

Conclusion

A novel chemical route for one-dimensional growth of InP QRs via reaction of metallic indium droplets and phosphide ions has been developed. This route should be of use when applied to other indium group-V semiconductor QRs. Preliminary results show that free-standing soluble InAs QRs can also be synthesized by the same procedure when $As(SiMe_3)_3$ is used instead of $P(SiMe_3)_3$. InP and InAs QRs synthesized by this procedure do not have residual metallic catalyst spherules at the rod tips, as is the case with previously prepared zinc blende III−V nanocrystals[11−14] when metallic particles are used as catalysts. The presence of metal is not desirable because it can change the electronic properties of QRs. High-quality QRs can be obtained only if the In^0 droplets are monodispersed and exist as a colloidal transparent solution at high temperature. Diluted solutions and low temperature (110−220 °C) are required for

(24) Liu, D.; Kamat, P. V. *J. Phys. Chem.* **1993**, *97*, 10769.
(25) Plass, R.; Pelet, S.; Krueger, J.; Grätzel, M.; Bach, U. *J. Phys. Chem. B* **2002**, *106*, 7578.
(26) Vogel, R.; Weller, H. *J. Phys. Chem.* **1994**, *98*, 3183.
(27) Zaban, A.; Micic, O. I.; Gregg, B. A.; Nozik, A. J. *Langmuir* **1998**, *14*, 3153.

the formation of soluble free-standing quantum rods with a small aspect ratio. Under these conditions, the diameter and length of the final QRs are self-limited at low temperature by the monodisperse In^0 droplets. A photoactive $InP-TiO_2$ composite was prepared by the same procedure. This procedure can be used for growing InP or other indium group-V semiconductor nanocrystals on various supporting materials in order to achieve better contact between nanocrystals and substrate. Exploration of the physical characteristics and optical properties of these InP QRs will continue.

Acknowledgment. This work was supported by the U.S. Department of Energy, Office of Science, Office of Basic Energy Sciences, Division of Chemical Sciences, Geosciences, and Biosciences.

JA039311A